Anomalous Gluon Self-Interactions and $t\bar{t}$ Production

Elizabeth H. Simmons* and Peter Cho**

Department of Physics, Boston University
590 Commonwealth Avenue, Boston MA 02215
*** Lauritsen Laboratory, California Institute of Technology*
Pasadena, CA 91125

Strong-interaction physics that lies beyond the standard model may conveniently be described by an effective Lagrangian. The only genuinely gluonic CP-conserving term at dimension six is the three-gluon-field-strength operator G^3. This operator, which alters the 3-gluon and 4-gluon vertices form their standard model forms, turns out to be difficult to detect in final states containing light jets. Its effects on top quark pair production hold the greatest promise of visibility.

INTRODUCTION

The hallmark of a non-abelian gauge theory is the self-interaction of its gauge fields. Most of this conference has been devoted to the electroweak vector bosons; this talk[1] will focus, instead, on the self-interactions of the gluons. Any experimental indication that the gluon self-coupling differed from the form predicted by the $SU(3)$ gauge theory of the strong interactions would point to the existence of new color-related physics. This talk presents a model-independent effective Lagrangian analysis of possible non-standard contributions to color physics, and assesses the possibility of measuring the coefficients of the effective Lagrangian.

Suppose that some exotic color physics exists at an energy scale Λ. For instance, there might be new colored scalars or fermions with a mass of order Λ, such as squarks and gluinos (1), colored technihadrons (2), or fermions in non-fundamental representations of $SU(3)$. Or instead, perhaps the gluons and quarks are manifestly composite (3) when probed at a distance scale Λ^{-1}. Such non-standard physics would lead to new gluon self-interactions through virtual loops of heavy colored particles or through exchange of sub-components.

A *complete* description of a given set of new phenomena would require a fundamental theory beyond the standard model. But at low energies $E << \Lambda$, where the underlying preon exchange or loops of new particles cannot be resolved, the new color physics causes multi-gluon contact interactions

---

[1]Presented by E.H. Simmons.

1

suppressed by inverse powers of Λ. These contact interactions are described by an effective Lagrangian

$$\mathcal{L}_{eff} = \mathcal{L}_{QCD} + \frac{1}{\Lambda^2}\sum_i C_i^{(6)}(\mu)O_i^{(6)}(\mu) + \frac{1}{\Lambda^4}\sum_i C_i^{(8)}(\mu)O_i^{(8)}(\mu) + O(\frac{1}{\Lambda^6})$$

(1)

that includes the conventional QCD Lagrangian plus non-renormalizable operators O_i that are constructed from gluon field strengths $G^{\mu\nu}$ or color-covariant derivatives $D^\mu = \partial^\mu - ig_sG^\mu$. The new operators obey the gauge and global symmetries of the standard model.

Our task is to identify the leading operators in this effective Lagrangian and determine which experiments are best able to detect their effects.

LEADING OPERATORS IN $\mathbf{L}_{EFF}$

Since a non-renormalizable operator of dimension $(4+d)$ is suppressed by Λ^{-d}, the operators making the most visible contribution to physical processes will be those of lowest dimension.

The number of nonrenormalizable terms which arise at dimension 6 in the gluon sector is small. One can build only two gauge-invariant operators preserving C, P and T out of covariant derivatives and gluon field strengths (5):

$$O_1^{(6)} = g_s f_{abc} G_{a\nu}^\mu G_{b\lambda}^\nu G_{c\mu}^\lambda$$

(2)

$$O_2^{(6)} = \frac{1}{2}D^\mu G_{\mu\nu}^a D_\lambda G_a^{\lambda\nu}.$$

(3)

The triple gluon field strength term in Eq. 2, which we shall name G^3 for short, represents a true gluonic operator, contributing to three-gluon and four-gluon non-abelian vertices. The double gluon field strength operator in Eq. 3, which we will call $(DG)^2$, is not really gluonic in this sense. The classical equation of motion

$$D_\mu G_a^{\mu\nu} = -g_s \sum_{\text{flavors}} \bar{q}\gamma^\nu T_a q$$

(4)

relates its S-matrix elements to those of a color octet four-quark operator (17):

$$O_2^{(6)} \xrightarrow{EOM} \frac{g_s^2}{2}\sum_{\text{flavors}}\left(\bar{q}\gamma_\mu T_a q\right)\left(\bar{q}\gamma^\mu T_a q\right).$$

(5)

The two-field-strength operator thus affects parton processes involving external quarks rather than external gluons.

The list of CP-even gluon operators grows significantly at dimension eight. Classifying the operators according to the number of field strengths that they

contain, we find one independent operator built from two field strengths and four covariant derivatives, two operators with three gluon field strengths and two derivatives, and a half-dozen operators containing four field strengths (6,9). Rather than listing all nine operators explicitly (for a list, see (6)) we merely mention that there are two situations in which dimension-8 operators may give noticeable effects. One of the two-field-strength operators,

$$O_3^{(8)} = g_s f_{abc} G_{a\nu}^\mu G_{b\lambda}^\nu D^2 G_{c\mu}^\lambda. \tag{6}$$

contributes at tree-level and order $1/\Lambda^4$ to the process $gg \to q\bar{q}$; it is the only $d = 8$ gluonic operator to do so. The effect of this operator on angular distributions will feature in our discussion of $gg \to t\bar{t}$. In addition, the four-field-strength operators contribute significantly to the gluon four-point vertex and, hence, the process $gg \to gg$ which we will analyze shortly.

DIJET PRODUCTION

Having established our operator basis, we consider how best to detect the presence of non-standard gluon self-interactions. In principle, the operator G^3, being the lowest-dimension operator to affect multi-point gluon vertices, is the one to focus on. A logical beginning is to consider its effects on hadronic scattering at high-energy colliders like FNAL and the LHC. Because scattering at both colliders is dominated by gluon-gluon collisions, one expects non-standard gluon self-interactions to noticeably affect two-body scattering cross-sections. These cross-sections, in turn, dominate the well-measured (at FNAL) inclusive single-jet production cross-section. Hence, it appears that a strong limit on the coefficient $C_1^{(6)}/\Lambda^2$ should be forthcoming.

The leading contribution of the G^3 operator to the inclusive jet cross-section $\mathbf{p}^{(\overline{\mathbf{p}})} \to \mathbf{jet} + \mathbf{X}$ is expected to lie in its effect on the sub-process $gg \to gg$. Consider the Feynman diagrams contributing to the $gg \to gg$ scattering amplitude in pure QCD and those with one insertion of G^3 (i.e., one anomalous multi-gluon vertex per diagram). The ordinary QCD contribution to the scattering comes from squaring the sum of the QCD diagrams; the lowest-order ($\frac{1}{\Lambda^2}$) piece due to G^3 arises from the interference of the QCD and one-insertion diagrams. It has been shown (5), however, that the QCD amplitude is only in the $[+ + ++]$ helicity channel and the one-insertion amplitude is purely in the orthogonal $[+ + --]$ and $[+ - --]$ channels. There is, consequently, no order $\frac{1}{\Lambda^2}$ contribution to $gg \to gg$. The leading effect of the G^3 operator arises at order $1/\Lambda^4$, from squaring the one-insertion diagrams and from interfering two-insertion diagrams with the QCD diagrams.

Where a lower-order effect is missing, one would hope to experimentally detect the remaining higher-order effect. This will be difficult. The leading contributions of the dimension-eight four-field-strength operators to $gg \to gg$ also arise at order $1/\Lambda^4$ when an amplitude with one insertion of a dimension-eight operator interferes with a QCD amplitude. Furthermore,

the order $1/\Lambda^4$ contributions to gluon scattering of the operators G^3 and $f_{eab}f_{ecd}G_a^{\mu\nu}G_b^{\lambda\rho}G_{c\mu\nu}G_{d\lambda\rho}$ are identical in form and similar in magnitude (6). Isolating the effects of G^3 in $gg \to gg$ does not appear possible.

The next most promising sub-processes appear to be those involving massless quarks as well as gluons, i.e. $gq \to gq$ and reactions related to it by crossing. Initial state gluons are still a possibility and G^3 can enter some diagrams through the three-gluon vertex. When the contribution of G^3 is calculated, however, the order $1/\Lambda^2$ piece vanishes. The leading effects are, again, order $1/\Lambda^4$ and compete with the effects of higher-dimension operators.

In summary: two-body scattering of massless partons does not put significant limits on non-standard gluon self-interactions involving the G^3 operator. Because the leading effects are of order $1/\Lambda^4$, there is competition from higher-dimension operators. Furthermore, the fact that gluons predominate at low x where the QCD background is greatest weakens the attainable bounds (6).

OTHER JET-PRODUCTION EXPERIMENTS

While the G^3 operator cannot be detected in $2 \to 2$ light parton scattering processes, there are several other options for studying non-standard strong interactions using massless final-state jets. As will become clear, none is fully satisfactory.

Although G^3 does not affect dijet production at tree level, the other dimension-six operator, $(DG)^2$ can. As noted earlier, this operator alters the propagator and coupling of internal gluons. At leading order its effects on scattering are equivalent to those of the four-quark operator $\left(\bar{\psi}\gamma^\mu T^a \psi\right)^2$. Consider, for example, the process $\mathbf{p\bar{p} \to jet + X}$, to which dijet production is the leading contributor. At FNAL, initial quarks play a larger role than initial gluons in scattering at large Bjorken x; thus high $p_\perp$ jets are more likely to originate from initial quarks. The inclusive jet cross-section is found to fall more slowly with $\hat{s}$ or $p_\perp$ when an insertion of the $(DG)^2$ operator is included than when only QCD is studied (5–7). This makes the transverse-momentum spectrum potentially sensitive to the presence of the $(DG)^2$ operator. Analyzing published CDF inclusive jet data (16) yields a lower bound of 2 TeV on the scale of new physics associated with this operator (7). This limit is useful – but because no external gluons are involved, it is only tangentially related to probing the structure of the gluon self-coupling.

At LEP, one source of 4-jet final states is the process wherein a Z decay to a quark/anti-quark pair is followed by radiation of a gluon that splits into a pair of gluons. The three-gluon vertex involved in this process can be affected by the presence of the G^3 operator. In (11,12) it was found that while most kinematic variables describing $Z \to 4j$ would reflect the presence of G^3 only in the overall *rate*, the dijet invariant mass distribution of the two most energetic jets changes *shape* when the G^3 operator is included. With 10pb^{-1} of data, it should be possible to set a limit of $\Lambda > 100$ GeV using this dijet invariant

mass distribution; ten times the data would boost the limit to 175 GeV. The limiting factor is the energy at which LEP experiments are performed.

While the order $1/\Lambda^2$ contributions of the G^3 operator to dijet production vanish at tree level, the same is not true when larger numbers of jets are being produced. The very difference in helicity properties between the scattering amplitudes of pure QCD and those with one insertion of G^3 which keeps the $2 \to 2$ amplitudes from interfering provides a potential signal of the presence of G^3 in $2 \to 3$ processes (10). For example, if one considers $gg \to ggg$ when two of the outgoing gluons are nearly collinear one observes the following. Treating the nearby gluons as one effective gluon yields an approximate $2 \to 2$ process for which we know the helicity properties of scattering amplitudes with and without G^3. The pure QCD amplitude with its $[++++]$ helicity is symmetric under azimuthal rotations about the momentum vector of the effective gluon. The amplitude with an insertion of G^3 admits the $[+ + --]$ and $[+ + +-]$ helicities which allows the effective gluon to be linearly polarized, yielding azimuthal dependence. No limits on Λ have yet been suggested using this method; the limiting factor may be the experimental difficulty of studying 3-jet events in the near-collinear region.

THE TOP QUARK PRODUCTION CROSS-SECTION

Light jets having failed us, we turn to the possibility of studying anomalous gluon self-interactions through their effects on scattering involving heavy flavors. The two-body scattering process that both involves heavy fermions and benefits maximally from the high gluon luminosity at hadron colliders is $gg \to q\bar{q}$. We will find that the order $1/\Lambda^2$ contribution of G^3 to this process is proportional to m_q^2; hence the effect is greatest for top production. The top quark is also the easiest to tag since its leptonic decay channel can produce a high energy, isolated lepton in conjunction with a bottom quark. This distinctive signature cuts down on genuine backgrounds as well as false identifications. To the extent that $b\bar{b}$ and even $c\bar{c}$ final states can be cleanly identified, the signal for G^3 will be enhanced and our results can be applied to their study.

To study top quark production, we must enlarge our basis of higher-dimension operators. The gluonic operators described above are not the only higher-dimension operators that can affect top production. They also do not form a closed basis under one-loop renormalization, which we employ in running down from the scale of new physics to the top production threshold. The operators $O_1^{(6)}$ and $O_2^{(6)}$ do not mix with each other under the action of QCD at one-loop order. Instead, $O_1^{(6)}$ runs into itself and the chromomagnetic moment operator

$$O_0^{(6)} = \sum_{\text{flavors}} g_s m_q \bar{q} \sigma^{\mu\nu} T^a q G_{\mu\nu}^a. \tag{7}$$

Because the equations of motion relate $O_2^{(6)}$ to a color-octet four-quark operator, $O_2^{(6)}$ mixes at one loop with other four-quark operators

$$O_3^{(6)} = \frac{g_s^2}{2} \sum_{\text{flavors}} \left(\bar{q}\gamma_\mu\gamma^5 T_a q\right)\left(\bar{q}\gamma^\mu\gamma^5 T_a q\right) \tag{8}$$

$$O_4^{(6)} = \frac{g_s^2}{2} \sum_{\text{flavors}} \left(\bar{q}\gamma_\mu q\right)\left(\bar{q}\gamma^\mu q\right) \tag{9}$$

$$O_5^{(6)} = \frac{g_s^2}{2} \sum_{\text{flavors}} \left(\bar{q}\gamma_\mu\gamma^5 q\right)\left(\bar{q}\gamma^\mu\gamma^5 q\right) \tag{10}$$

The mixing matrices are given explicitly in (8,9).

Renormalization group evolution suppresses the coefficients $C_1^{(6)}$ and $C_2^{(6)}$. Given that one expects some new fundamental layer of physics to lie in the TeV regime, we will take $\Lambda =$2 TeV. This ensures that our analysis will be valid over almost the entire energy range of present and anticipated hadron colliders. If the operator coefficients assume the values

$$(C_0^{(6)}, C_1^{(6)}, C_2^{(6)}, C_3^{(6)}, C_4^{(6)}, C_5^{(6)})(\Lambda) = (1, 1, 1, 0, 0, 0) \tag{11}$$

at a scale of 2 TeV, then they run down to the values

$$(0.7858, 0.7458, 0.8856, -0.0294, 0.0003, -0.0152) \tag{12}$$

at the top-antitop threshold (8).

The partonic sub-processes contributing to top quark pair-production at a hadronic collider are $gg \to t\bar{t}$ and $q\bar{q} \to t\bar{t}$. Both the G^3 and chromomagnetic moment operators contribute to the gluon fusion channel; the non-standard contribution to the squared matrix element is

$$\overline{\sum}{}' \mid \mathcal{A}(gg \to t\bar{t})|^2 = \frac{m_t^2}{\Lambda^2}\left[\frac{C_0^{(6)}(\frac{4}{3}\hat{s}^2 - 3\hat{t}\hat{u} - 3m_t^2\hat{s} + 3m_t^4) + \frac{9}{8}C_1^{(6)}(\hat{t} - \hat{u})^2}{(m_t^2 - \hat{t})(m_t^2 - \hat{u})}\right]$$
$$+ \frac{1}{\Lambda^4}\left[\frac{1}{6}C_0^{(6)\,2}\frac{m_t^2\left(14\hat{s}\hat{t}\hat{u} + m_t^2(31\hat{s}^2 - 36\hat{t}\hat{u}) - 50m_t^4\hat{s} + 36m_t^6\right)}{(m_t^2 - \hat{t})(m_t^2 - \hat{u})}\right. \tag{13}$$
$$\left. + \frac{9}{8}C_0^{(6)}C_1^{(6)}\frac{m_t^2\hat{s}^3}{(m_t^2 - \hat{t})(m_t^2 - \hat{u})} + \frac{27}{4}C_1^{(6)\,2}(m_t^2 - \hat{t})(m_t^2 - \hat{u})\right] + O\left(\frac{1}{\Lambda^6}\right).$$

where the bar over the Σ implies averaging (summing) over initial (final) spins and colors, while the prime indicates division by g_s^4. Notice that all of the nonrenormalizable operator terms except the last one are proportional to m_t^2. Because the last term is enhanced by a prefactor of $27/4$ and increases quadratically with $\hat{s}$, well away from the $t\bar{t}$ threshold and over large regions of $C_1^{(6)}$ parameter space, the $O_1^{(6)}$ operator's squared amplitude is much larger than its interference with QCD.

One may question whether the $O(1/\Lambda^4)$ terms arising from dimension-8 gluon operators could be significant. The answer is generally no. The only dimension-8 operator that affects $gg \to t\bar{t}$ scattering at lowest order is $O_3^{(8)}$

$$\overline{\sum}{}' |\mathcal{A}(gg \to t\bar{t})|^2 = \cdots - - - \frac{3}{8} \frac{C_3^{(8)}}{\Lambda^4} \frac{m_t^2 \hat{s}(\hat{t} - \hat{u})^2}{(m_t^2 - \hat{t})(m_t^2 - \hat{u})}. \tag{14}$$

This term has a smaller prefactor and increases more slowly with $\hat{s}$ than the term proportional to $(C_1^{(6)})^2$ and is unlikely to obscure any signal from $O_1^{(6)}$.

The $(DG)^2$, chromomagnetic moment, and four-quark operators make the following addition to the quark/anti-quark annihilation matrix element

$$\overline{\sum}{}' \mid \mathcal{A}(q\bar{q} \to t\bar{t})|^2 = \tag{15}$$

$$\frac{1}{9\hat{s}\Lambda^2} \left[4C_0^{(6)} m_t^2 \hat{s} + C_2^{(6)}(\hat{t}^2 + \hat{u}^2 + 4m_t^2 \hat{s} - 2m_t^4) + C_3^{(6)} \hat{s}(\hat{t} - \hat{u}) \right]$$

$$+ \frac{4}{9\Lambda^4} \left[8C_0^{(6)2} m_t^2(\hat{t}\hat{u} + 2m_t^2\hat{s} - m_t^4)/\hat{s} + 8C_0^{(6)}C_3^{(6)} m_t^2(\hat{t} - \hat{u}) \right.$$

$$+ 8C_0^{(6)}C_2^{(6)} m_t^2 \hat{s} + (C_2^{(6)2} + \frac{1}{2}C_4^{(6)2})(\hat{t}^2 + \hat{u}^2 + 4m_t^2\hat{s} - 2m_t^4)$$

$$\left. + (C_3^{(6)2} + \frac{1}{2}C_5^{(6)2})(\hat{t}^2 + \hat{u}^2 - 2m_t^4) + (2C_2^{(6)}C_3^{(6)} + C_4^{(6)}C_5^{(6)})\hat{s}(\hat{t} - \hat{u}) \right].$$

with the same conventions as before. Unlike Eq. 13 this expression contains no anomalously large order $1/\Lambda^4$ term. So we expect the effect of dimension-eight and higher operators upon $q\bar{q} \to t\bar{t}$ scattering to be small (8).

The squared amplitudes in Eqs. 13 and 15 enter the partonic cross section

$$\frac{d\sigma(ab \to t\bar{t})}{d\hat{t}} = \frac{\pi\alpha_s^2}{\hat{s}^2} \overline{\sum}{}' |\mathcal{A}(ab \to t\bar{t})|^2 \quad . \tag{16}$$

This is combined with distribution functions $f_{a/A}(x_a)$ and $f_{b/B}(x_b)$ specifying the probability of finding partons a and b inside hadrons A and B carrying momentum fractions x_a and x_b and summed over initial parton configurations. The resulting hadronic cross section

$$\frac{d^3\sigma}{dy_3 dy_4 dp_\perp}(AB \to t\bar{t}) = 2p_\perp \sum_{ab} x_a x_b f_{a/A}(x_a) f_{b/B}(x_b) \frac{d\sigma(ab \to t\bar{t})}{d\hat{t}}. \tag{17}$$

depends on the top and antitop rapidities y_3 and y_4 and their common transverse momentum $p_\perp$.

TOP QUARK PRODUCTION AND GLUON SELF-INTERACTIONS

We now compare the effects of various non-standard gluon interactions on the top quark production cross-section. This discussion will communicate

the conclusions that can be drawn from the salient features of the kinematic distributions of the top quarks. Full details reside in (8).

We first examine the transverse momentum distribution obtained by integrating $d^3\sigma/dy_3 dy_4 dp_\perp$ over the rapidity range $-2.5 \leq y_3, y_4 \leq 2.5$. [2] The resulting $p_\perp$ distribution of $t\bar{t}$ pairs produced at the LHC is plotted in Fig. 1, which shows curves for QCD and for the separate contributions of operators $O_0^{(6)}$, $O_1^{(6)}$ and $O_2^{(6)}$ with their respective $C_i(\Lambda)$ equal to 0.5. [3]

FIG. 1. $d\sigma(pp \to t\bar{t})/dp_\perp$ at the LHC with $\sqrt{s} = 14$ TeV. The solid curve represents pure QCD. The dot-dashed, dashed and dotted curves show the additional contributions when either $C_0^{(6)}(\Lambda)$, $C_1^{(6)}(\Lambda)$ or $C_2^{(6)}(\Lambda)$ is set to 0.5 with $\Lambda = 2$ TeV.

The $p_\perp$ dependence of the curves in Fig. 1 differentiates the dimension-6 operators from each other and from QCD terms in $\mathcal{L}_{eff}$. At high $p_\perp$, where the QCD background is lowest, the dimension-6 operator making the largest contribution to the rate of top quark production is G^3. Next in importance at large $p_\perp$ is $(DG)^2$; the chromomagnetic magnetic operator lags far behind. Placing a lower $p_\perp$ cut around 500 GeV, can eliminate most of the chromomagnetic moment operator's contribution in favor of that from G^3 and $(DG)^2$. In addition, the shapes of the curves for G^3 and $(DG)^2$ are noticeably different from one another and from the shape of the QCD curve; that

---

[2]This convenient integration interval contains the bulk of the produced top quarks. Extending the range to $-6 \leq y_3, y_4 \leq 6$ does not alter our results.

[3]We used the next-to-leading order parton distribution function set B of Harriman, Martin, Roberts and Stirling (18) evaluated at the $\mu = m_\perp \equiv \sqrt{m_t^2 + p_\perp^2}$.

of the chromomagnetic moment operator closely mimics QCD. Hence the G^3 operator should make the most visible contribution to $d\sigma/dp_\perp$ at the LHC.

A quantitative comparison of the QCD and effective lagrangian predictions for $d\sigma(pp \to t\bar{t})/dp_\perp$ at the LHC confirms this (8). To compare rates, we computed the ratio $R_\perp$ of the integrals of $d\sigma_{EFT}/dp_\perp$ and $d\sigma_{QCD}/dp_\perp$ over the momentum range 500 GeV $< p_\perp <$ 1000 GeV. We found that $R_\perp$ was fairly insensitive to $C_0^{(6)}$, and depended a few times more strongly on $C_1^{(6)}$ than on $C_2^{(6)}$. To compare shapes, we formed a χ^2 function for the difference in number of high-$p_\perp$ events predicted by QCD and $\mathcal{L}_{eff}$. Again, the strongest dependence was on $C_0^{(6)}$. Further, $R_\perp$ and the χ^2 function depend differently on $C_1^{(6)}$ and $C_2^{(6)}$, making the combined measurements even more powerful. We estimate that the LHC could set a limit $|C_1^{(6)}| < 0.5$.

The Tevatron analogues of the LHC differential cross-sections are shown in Fig. 2. The integrated cross-section for $t\bar{t}$ production is two orders of mag-

FIG. 2. $d\sigma(p\bar{p} \to t\bar{t})/dp_\perp$ at FNAL with $\sqrt{s} = 1.8$ TeV. The curves are labeled as in Fig. 1.

nitude lower at the Tevatron. And the relative importance of the dimension-6 terms in the effective Lagrangian depends upon $\sqrt{s}$ in a manner consistent with the parton content of the colliding hadrons. The most important dimension-six operators at Tevatron energies are the chromomagnetic moment operator $O_0^{(6)}$ and four-quark operators like $(DG)^2$; the effects of G^3 are (for equal values of the C_i at high energies) an order of magnitude smaller. Hence FNAL experiments are unlikely to find evidence for the G^3 operator in $t\bar{t}$

production. The effects of $O_0^{(6)}$ and $O_2^{(6)}$ may be visible in terms of enhanced production *rate*; again, the fact that the shape of the $O_0^{(6)}$ curve is identical to that of the QCD curve will make $O_0^{(6)}$ more difficult to detect.

We next study the angular distribution of the produced top quarks, $d\sigma(pp \to t\bar{t})/d\cos\theta^*$, where θ^* denotes the angle between the direction of the boost and that of the top quark in the parton center-of-mass frame. To enhance the signal we have imposed the cut $p_\perp \geq 500$ GeV. We also required the lab frame angle between the t or $\bar{t}$ and the beamline to exceed 25.4°; this ensures that the pseudorapidities of the decay products from high momentum tops will predominantly fall within $-2.5 \leq \eta \leq 2.5$, the approximate acceptance of planned LHC detectors .

The angular distribution is plotted in Fig. 3 for pure QCD and for QCD *plus* some of the O_i. The curves indicating the effects of the chromomagnetic

FIG. 3. $d\sigma(pp \to t\bar{t})/d\cos\theta^*$ at the LHC with $\sqrt{s} = 14$ TeV. The solid curve shows pure QCD. The dotted curve shows QCD plus $O_1^{(6)}$ with $C_1^{(6)}(2 \text{ TeV}) = 0.5$. The dashed (dot-dashed) curve shows QCD plus $O_3^{(8)}$ with $C_3^{(8)}(2 \text{ TeV}) = 0.5$ (-0.5).

moment operator are not included in the figure because they closely trace the QCD curve for $C_0^{(6)}(\Lambda) = \pm 0.5$. Likewise, the curves for $C_1^{(6)}(\Lambda) = -0.5$ and $C_2^{(6)}(\Lambda) = 0.5$ are nearly indistinguishable from the curve shown for

$C_1^{(6)}(\Lambda) = 0.5$. The dimension-8 gluon operator $O_3^{(8)}$ induces deviations [4] from pure QCD which are clearly visible in $d\sigma/d\cos\theta^*$. This is quite interesting since the effect of $O_3^{(8)}$ upon the $t\bar{t}$ transverse momentum distribution was negligible. Indeed, we omitted the effects of $O_3^{(8)}$ from Fig. 1 and Fig. 2 since they would have been suppressed relative to the dimension-6 operators' effects by more than an order of magnitude.

As in the analysis of the $p_\perp$ distributions, we distinguish between effects on the rate and the shape of the curves. In discussing rate, we compare the integral of a given curve (with respect to $\cos\theta^*$) to that of the QCD curve, denoting the ratio by R_{ang}. A curve's shape is compared with that of the QCD curve by forming the ratio (R_{rms}) of the respective root-mean-squared values of $\cos\theta^*$. For the curves arising when $C_0^{(6)}(\Lambda)$, $C_1^{(6)}(\Lambda)$, $C_2^{(6)}(\Lambda)$ or $C_3^{(8)}(\Lambda)$ is set equal to 0.5, we find $R_{\mathrm{ang}} = (1.03, 1.23, 1.46, 0.82)$ and $R_{\mathrm{rms}} = (0.999, 0.978, 0.991, 0.871)$. For analogous curves with the Λ scale coefficients set equal to -0.5, we find $R_{\mathrm{ang}} = (0.969, 1.23, 0.735, 1.18)$ and $R_{\mathrm{rms}} = (1.00, 0.978, 1.03, 1.08)$. The most striking implication is that the dimension-8 gluon operator alters the shape of the $t\bar{t}$ angular distribution more than any dimension-6 operator in $\mathcal{L}_{eff}$ for comparable values of the C_i. The magnetic moment operator's angular distribution is indistinguishable from that of pure QCD, while the distributions of the G^3 and $(DG)^2$ operators differ significantly from that of QCD in R_{ang} but not in R_{rms}.

Figure 4 summarizes the detectability of the operators we have studied. Each operator produces visible effects in a unique combination of experiments.

FIG. 4. Experiments able to detect each type of non-standard gluon interaction.

---

[4] The coefficient $C_3^{(8)}$ was not evolved using the renormalization group but was instead simply fixed at its Λ scale value.

CONCLUSIONS

Anomalous gluon self-interactions are elusive. Detecting them in dijet production is nearly impossible. Other measurements involving light jets are energy-limited or intrinsically difficult.

Heavy flavor production may offer the best hope of seeing non-standard gluon self-couplings. While only $t\bar{t}$ production is analyzed here, $b\bar{b}$ production should show similar effects. A strong signal will be provided by the shape of the transverse-momentum distribution of the produced heavy quarks; non-standard strong interactions can visibly affect the number of events at high transverse momentum. The angular distribution of the heavy fermions can also help discriminate among the effects of different higher-dimension operators.

Top-quark pair production at the LHC will test the three-gluon vertex well. The contribution of the G^3 operator to the transverse-momentum spectrum exceeds that of all other contact operators for similar values of their coefficients. For a scale of new physics $\Lambda = 2\text{TeV}$, LHC experiments should be able to set an upper bound of 0.5 on the coefficient of the G^3 operator. Using the more usual notation in which the coefficient C_i is set to 4π, the associated lower bound on Λ is of order 10 TeV. This compares well with the current lower bounds of order 1-2 TeV derived from FNAL data for both the 4-quark operator $(\bar{\psi}_L \gamma^\mu \psi_L)^2$ (16) and the $(DG)^2$ operator (7).

REFERENCES

1. P. Fayet, Nucl. Phys. B**90**, 104 (1975) and Phys. Lett. B**69**, 489 (1977); G.R. Farrar and P. Fayet, Phys. Lett. B**76**, 575 (1978); E. Witten, Nucl. Phys. B**188**, 513 (1981); S. Dimopoulos and H. Georgi, Nucl. Phys. B**193**, 150 (1981); N. Sakai, Z. Phys. C**11**, 153 (1981); L. Ibañez and G. Ross, Phys. Lett. B**105**, 439 (1981); R.K. Kaul, Phys. Lett. B**109**, 19 (1982); M. Dine, W. Fischler and M. Srednicki, Nucl. Phys. B**189**, 575 (1981); S. Dimopoulos and S. Raby, Nucl. Phys. B**192**, 353 (1981).
2. S. Weinberg, Phys. Rev. D**19**, 1277 (1979); L. Susskind, Phys. Rev. D**20**, 2619 (1979); E. Farhi and L. Susskind, Phys. Rep. **74**, 277 (1981).
3. See e.g. the review by M. Peskin in *Proceedings of the International Symposium on Lepton and Photon Interactions at High Energies, Bonn, 1981* edited by W. Pfeil (Physikalisches Institut, Universität Bonn, 1981), p. 880.
4. E. Eichten, K. Lane and M. Peskin, Phys. Rev. Lett. **50**, 811 (1983).
5. E.H. Simmons, Phys. Lett. B**226**, 132 (1989).
6. E.H. Simmons, Phys. Lett. B**246**, 471 (1990).
7. P. Cho and E.H. Simmons, Phys. Lett. B**323**, 401 (1994). hep-ph/9307232.
8. P. Cho and E.H. Simmons, Phys. Rev. D (1995). To appear. hep-ph/9408206.
9. A.Y. Mozorov, Sov. J. Nucl. Phys. **40**, 505 (1984); S. Narison and R. Tarrach, Phys. Lett. B**125**, 217 (1983).
10. L. Dixon and Y. Shadmi, Nucl. Phys. B**423**, 3 (1994).
11. H. Dreiner, A. Duff and D. Zeppenfeld, Phys. Lett. B**282**, 441 (1992).

12. A. Duff and D. Zeppenfeld, Z. Phys. C**53**, 529 (1992).

13. D. Atwood, A. Kagan and T. Rizzo (1994). hep-ph/9407408.

14. C. Hill and S. Parke, Phys. Rev. D**49**, 4454 (1994). hep-ph/9312324.

15. T. Rizzo, Phys. Rev. D**50**, 4478 (1994), hep-ph/9405391; T. Rizzo (1994). hep-ph/9407366.

16. CDF Collaboration, F. Abe et al., FERMILAB-PUB-91/231-E; Phys. Rev. Lett. **68**, 1104 (1992).

17. H.D. Politzer, Nucl. Phys. B**172**, 349 (1980).

18. P. Harriman, A. Martin, R. Roberts and J. Stirling, Phys. Rev. D**42**, 798 (1990).

$\cos \theta^*$
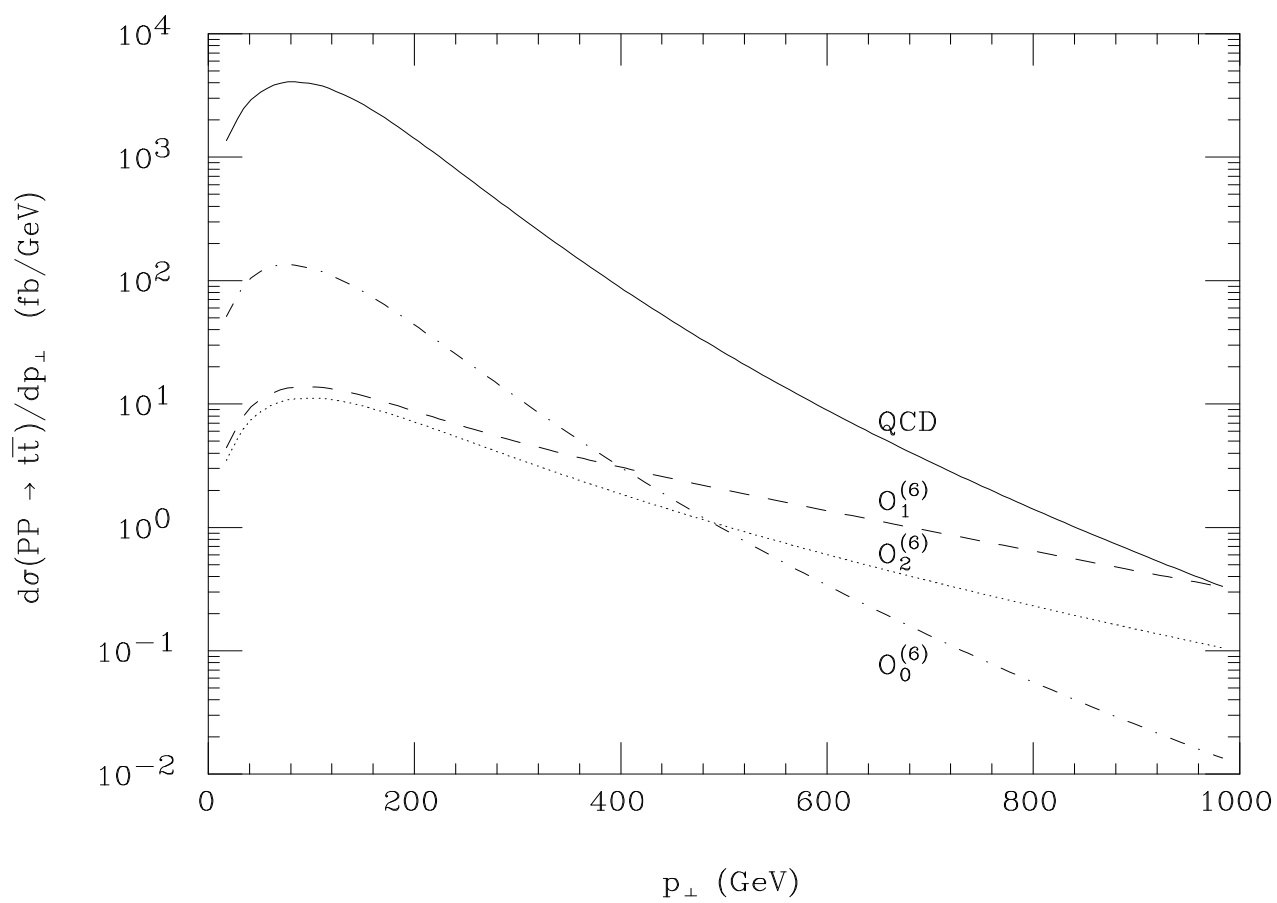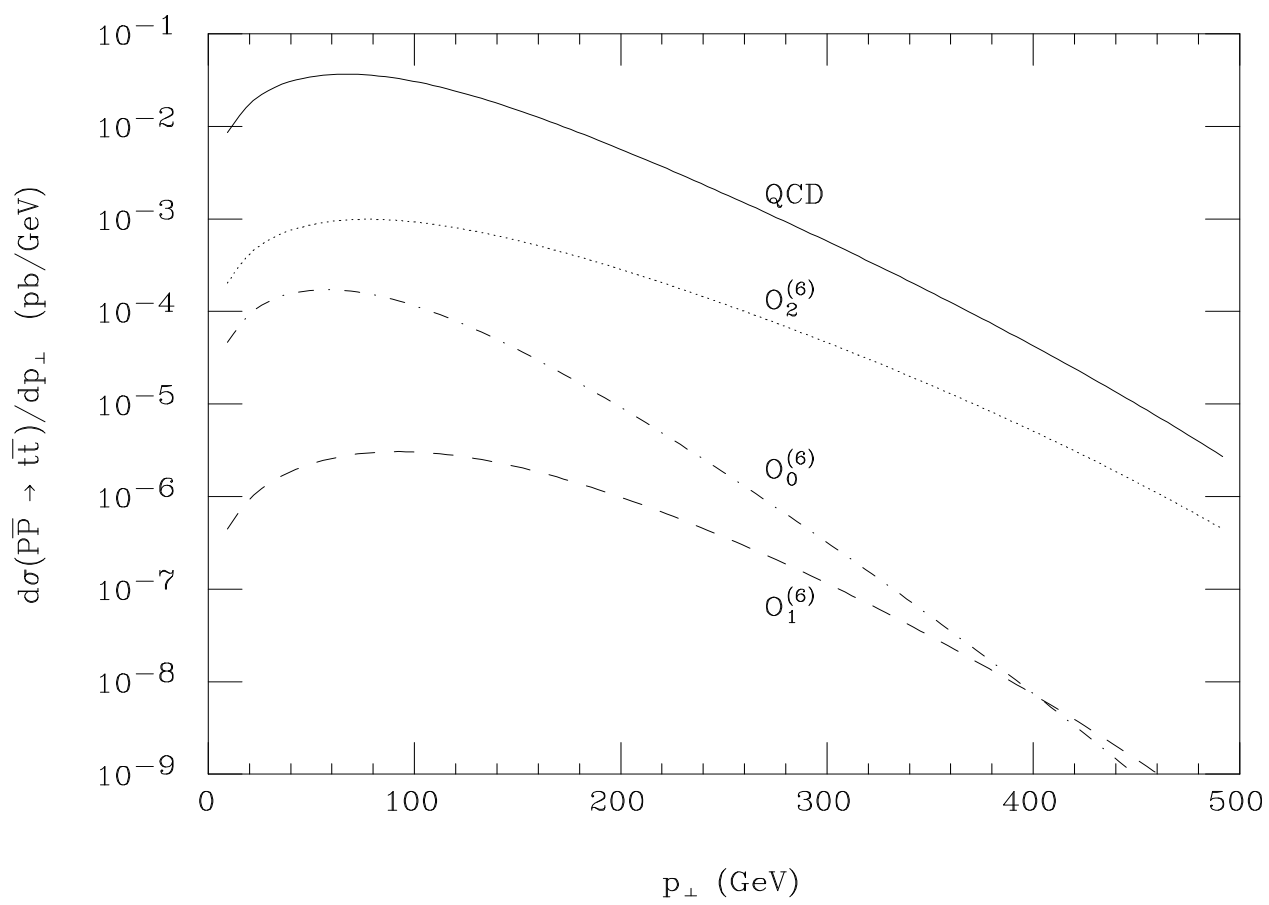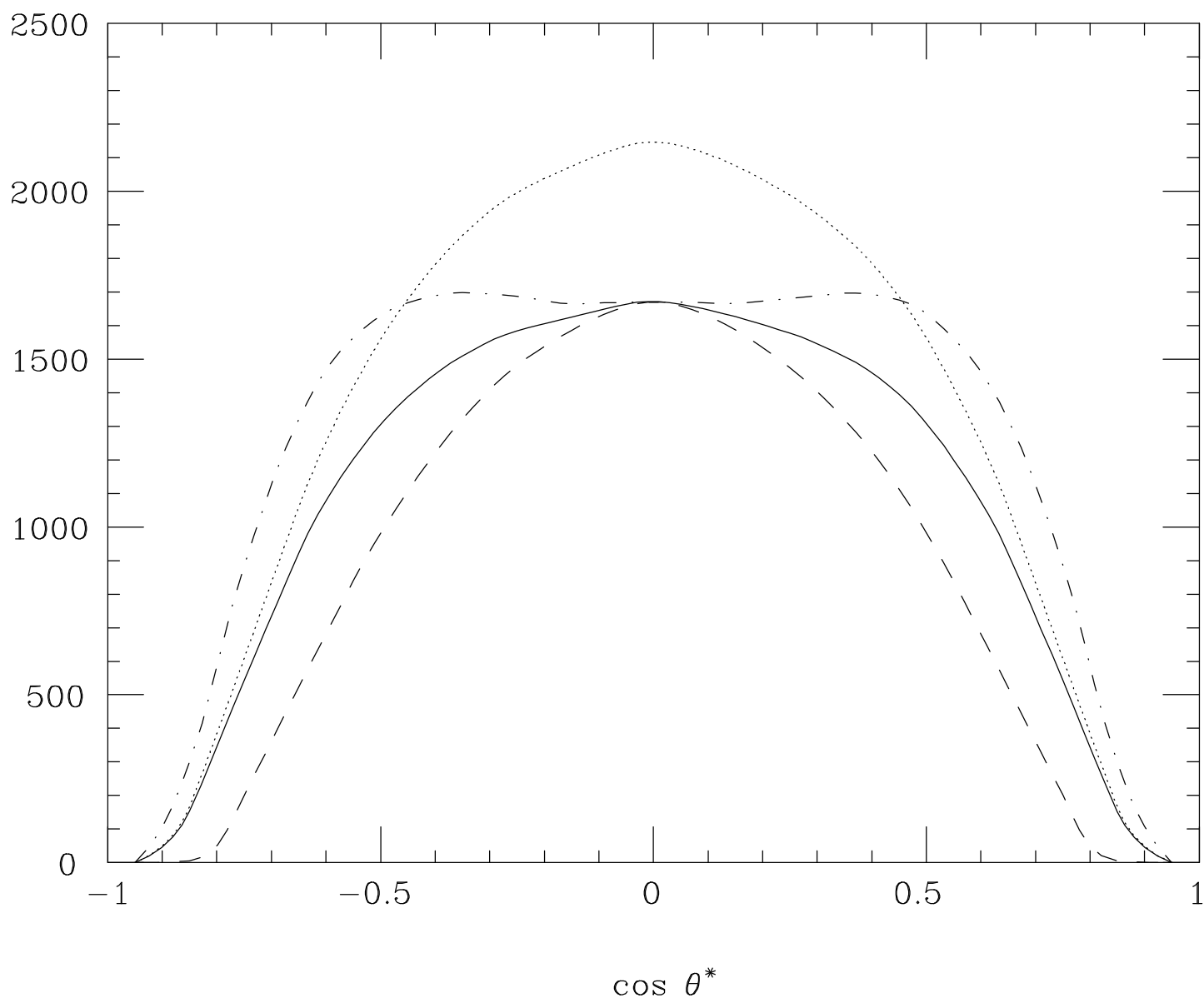
OPERATOR	EXPERIMENT				
	FNAL p_T	LHC p_T rate	p_T shape	angular rate	angular shape
$O_1^{(6)}$		√	√	√	
$O_2^{(6)}$	√	√	√	√	
$O_0^{(6)}$	√	√			
$O_3^{(8)}$				√	√